ELSEVIER

Journal of Nuclear Materials 248 (1997) 428–434

journal of nuclear materials

Investigation of hydrogen covered crystalline surfaces by low-energy ion-scattering and recoiling spectroscopy

O. Grizzi *, J.E. Gayone, G.R. Gómez, R.G. Pregliasco, E.A. Sánchez

Centro Atómico Bariloche and Instituto Balseiro, Comisión Nacional de Energía Atómica and Consejo Nacional de Investigaciones Científicas y Técnicas, 8400 San Carlos de Bariloche, Rio Negro, Argentina

Abstract

We describe the use of ion-scattering and recoiling spectroscopy to obtain information about the adsorption of hydrogen on crystalline surfaces. Examples of H coverage, surface atomic structure, adsorption sites and ion-surface electron exchange processes in the presence of surface hydrogen are discussed for the GaAs(110) and W(211) surfaces. © 1997 Elsevier Science B.V.

PACS: 82.65.My; 68.35.Bs; 79.20.Rf

1. Introduction

Neutral atom and ion beams in a very broad energy range (from thermal to MeV [1,2]) have been frequently used to characterize different aspects of the hydrogen–solid interaction. In particular, ions at keV energies are efficiently scattered by the ion cores of the substrate atoms and produce fast recoils (including hydrogen) [3,4] that can be detected together with the scattered projectiles to obtain information about the elemental composition and the atomic structure of the top and subsurface atomic layers. This technique is generically named as ion-scattering spectroscopy (ISS) or low-energy ion-scattering (LEIS) when only the scattered projectiles are detected, and direct recoiling spectroscopy (DRS) when the recoils are detected.

The use of ISS and DRS for surface analysis and the advantages of the techniques that have outgrown from them have been described in detail in several reviews [5–12]. In the present work, we discuss the information the technique provides about H adsorption on crystalline surfaces, in particular we describe examples of coverage monitoring, changes in the atomic structure of the substrate, adsorption sites and the effect of the surface H on the neutralization of backscattered projectiles.

* Corresponding author. Fax: +54-944 45 299; e-mail: grizzi@cab.cnea.edu.ar.

2. Experimental requirements

The basic requirement for ion scattering and recoiling spectroscopy are a 1–10 keV ion beam, a precision sample manipulator and energy analysis of the scattered and/or recoiled particles with a resolution $\lesssim 1\%$ by means of electrostatic analyzers [12,13] or time-of-flight (TOF) methods [14,15]. In most cases the sample must be in UHV; however in some recent applications ISS and DRS have been successfully used to monitor the growth of thin films at pressures of the order of 0.1 Pa [12]. If only the backscattered particles are detected, the beam line and a coaxial TOF detector system [16] can be mounted in a minimum of space using only one chamber port [17]. In order to detect the recoiled particles a TOF line or an electrostatic analyzer has to be mounted at forward angles, typically between 25° and 60° of scattering angle. In this case a TOF detector system allowing continuous variation of the observation angle is useful to optimize the separation between the scattering and the different recoil peaks [18,19]. The spectra shown in this work have been acquired either with the instrument described in Refs. [18,19] or with a basic UHV system [20] and a TOF analyzer mounted at a 107° scattering angle [21].

There are two major advantages in using TOF methods: first, the intensity of the direct recoil (DR) peaks are independent of neutralization effects, and second, the use of a multichannel detection method to measure both the

PII S0022-3115(97)00138-4

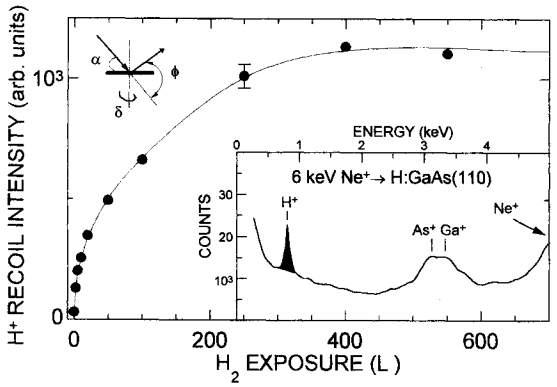

Fig. 1. H^+ forward recoil intensity induced for a H:GaAs(110) surface vs. H_2 exposure. Inset: typical forward recoiling spectrum induced by 6 keV Ne^+.

ions and neutrals enhances the efficiency of the technique, reducing the bombarding doses required to obtain a spectrum to 10^{15}–10^{16} projectiles/m^2. At this doses the damage produced in most surfaces is usually negligible. However, the continuous use of the technique may result in the deterioration of the surface of some compound semiconductors that cannot be annealed to high temperature to prevent changes in the surface stoichiometry. For the GaAs(110) surface this effect has been minimized by smoothing out the surface with repeated cycles of grazing ion bombardment and annealing [21]. This preparation method is efficient to clean the GaAs(110) surface and at the same time to improve the surface flatness. The W(211) surface was cleaned by prolonged annealing at 2300 K. The cleanliness of both surfaces was monitored by DRS and Auger electron spectroscopy (AES). No C or O contamination was detectable with these techniques after the cleaning procedures.

3. Monitoring the hydrogen coverage

One of the important capabilities of DRS is its high sensitivity to surface H ($\sim 10^{-3}$ of a monolayer (ML)), allowing direct monitoring of the H coverage in adsorption experiments and in film growth, something that cannot be done with most other surface analysis techniques. Many applications of surface H detection by DRS have been described in two recent reviews [11,12]. The direct detection of H is particularly important in cases where the adsorption requires the previous dissociation of the H_2 molecule (GaAs(110) for example), making difficult both the comparison of exposures performed in different equipments and the determination of saturation doses. The inset in Fig. 1 shows the energy distribution of the positive ions emitted during 6 keV Ne^+ bombardment of a GaAs(110) surface exposed to 500 L of H_2 (in the presence of a hot filament, 1 L = 1.33×10^{-4} Pa s). The spectrum was acquired with a custom made single-pass cylindrical mirror analyzer having a movable entrance slit positioned to select a scattering angle $\phi = 27°$ [20]. Adsorbed H, together with Ga and As emitted as positive ions in DR sequences are identified in the spectrum. The H DR peak appears superimposed to the high energy tail of sputtered ions, only the low energy tail of the scattered Ne^+ peak is seen.

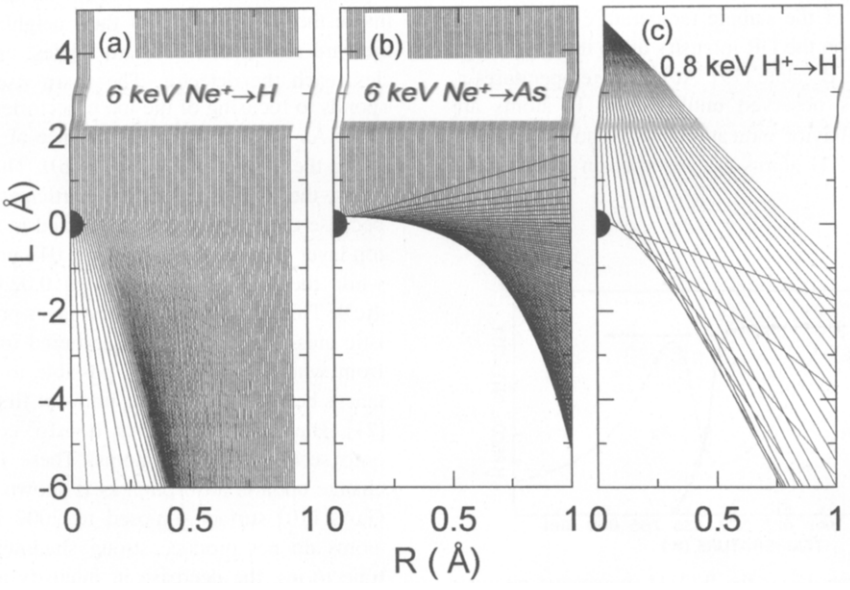

Fig. 2. Shadow cones formed behind H (a) and As (b) atoms for a Ne^+ parallel beam. (c) Blocking cone behind a H atom for H DR trajectories.

The area of the H^+ peak obtained from spectra similar to that shown in the inset is presented in Fig. 1 as a function of the H_2 exposure. Its non linear dependence suggests that the adsorption does not proceed with a sticking coefficient of 1 until saturation (independent of the dose), as it has been suggested previously [22]. The use of the H^+ DR peaks as representative of the H coverage requires some consideration. First, since in this experiment only the H^+ ions are measured, we have to assume that the neutralization rate for the emitted H^+ is independent of the dose. This should be a good approximation, at least at low coverage, where the H–H interaction is small and the electronic structure around each H atom should be basically the same. Second, the incidence and observation angles should be sufficiently large to avoid modifications of the Ne incoming or H outgoing trajectories by shadowing, focusing or blocking effects. These effects are shown in Fig. 2 by trajectory simulations [21] of 6 keV Ne–As and Ne–H collisions, considering parallel incoming trajectories, and for 0.8 keV H–H collisions in outgoing divergent trajectories. The incidence angle (α) and the observation angle (ϕ) used to acquire the spectrum of Fig. 1 were chosen large enough ($\alpha = 8.5°$ and $\phi = 27°$) so that even at a full ML coverage all the H atoms are outside the shadowing or blocking regions cast by their neighbors. When this condition cannot be fulfilled, a calibration of the masking effects becomes necessary [23].

Another use of DRS is the monitoring of the H coverage as a function of the sample temperature. Fig. 3 shows the variation of the H DR intensity for a H saturated W(211) surface as a function of the surface temperature, together with the flash desorption spectrum [19,24]. These H DR intensities were obtained from TOF spectra of neutrals plus ions produced by 4 keV Ne^+ bombardment [19]. The increase of the sample temperature from 300 K produces no effect on the DR intensity up to the desorption temperature for the β_2 state [19]. At higher temperatures a strong decrease is observed until all the H atoms are desorbed. This behavior indicates that at and above room temperature all the H atoms are adsorbed in the β_2 state.

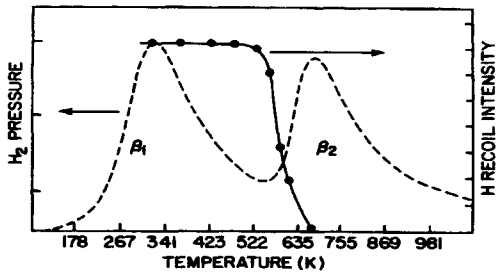

Fig. 3. H recoil intensity vs. the W(211) temperature measured with 4 keV Ar^+ ions and flash desorption spectrum from Refs. [19,24].

4. Monitoring the adsorbate and substrate atomic structure

The experimental determination of the adsorbate and substrate atomic structures is crucial for testing models describing the H-surface interaction. As we have seen in Fig. 2, the H atom produces a relatively small deviation of the projectile trajectories, thus the H adsorbed layer can be considered quite transparent for the projectiles going in and out of the surface. If the atomic structure of the clean surface can be described well by ISS, the changes induced by the H adsorption should also be described with a similar accuracy. Substrates composed of heavy target atoms ($Z \geq 20$) are the best candidates [25–27]. This should not be considered too restrictive, characterization of H:Si(100) based on the analysis of Si and adsorbate recoils has been recently reported [28,29].

Most of the information about the substrate surface structure is obtained from the analysis of the projectile intensity backscattered at large angles ($\geq 90°$) as a function of the glancing (α) and azimuthal (δ) incidence direction [6,7]. The inset of Fig. 4(a) shows an example of a TOF spectrum of ions plus neutrals acquired for 6 keV Ne^+ backscattering from a clean GaAs(110) surface along $\delta = 64.7°$. The incidence and scattering angles were set at $\alpha = 8.5°$ and $\phi = 107°$, respectively. The two major peaks come from quasi-single scattering from As and Ga atoms, the latter being broader because of the similar abundance of the ^{69}Ga and ^{71}Ga isotopes. The shoulder at lower TOF and the long tail at large TOF are the contributions of multiple scattering. The quasi-single backscattering intensity coming from As atoms $I_{BS}(As)$ (shaded area in the spectrum) change with the incidence angle as is shown in Fig. 4(a). At very low α ($< 3°$) all the target atoms are inside the shadow cone of their neighbor and the projectiles are scattered at forward angles; essentially no particles reach the detector. The sharp rise at $\alpha = 4°$ corresponds to focusing of the ion trajectories onto As atoms by other As atoms sitting at a distance of 1.87 nm (measured along the dashed line in Fig. 4(b)). The Ga atoms that lie along the trajectory do not participate in the scattering because the clean surface is relaxed in such a way that the top layer Ga atoms are shifted 0.043 nm towards the bulk, while the As atoms are shifted 0.023 nm up [21] (Fig. 4(c)). This splitting of the first layer produces a characteristic anisotropy in the backscattered intensity distribution, from whose analysis it is possible to determine the distances between Ga and As atoms of first and second layers [21]. The rise in $I_{BS}(As)$ at $\alpha = 16°$ comes from focusing onto second layer As atoms. These features in $I_{BS}(As)$ change upon H adsorption as is shown in Fig. 4(a) for the GaAs(110) surface exposed to 2000 L of H_2. Since H atoms do not produce strong shadowing of the incident trajectories, the decrease in intensity and the shift of the first layer focusing is a clear evidence of the change in the surface atomic structure. In this case the surface derelaxes

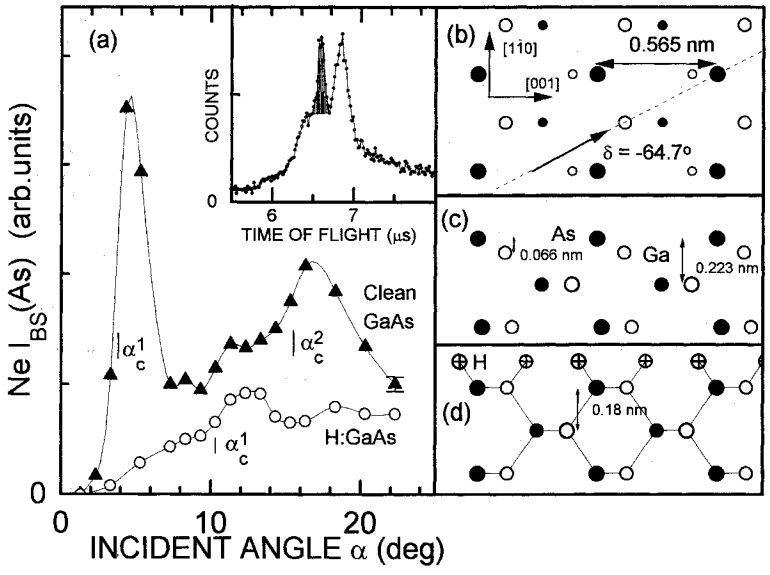

Fig. 4. (a) Neutral plus ion intensity for 6 keV Ne backscattering from top layer As atoms in the clean and hydrogenated GaAs(110) surface (shaded area in the spectrum) vs. the glancing angle. (b) Top and (c) side views of the clean (relaxed) surface. (d) Side view of the bulk terminated surface with adsorbed H.

towards a termination close to that of the bulk as is shown in Fig. 4(d). The top layer Ga atoms sit at the same height as the As atoms. As a result, the focusing effect is shifted to larger incident angles and, since the distance between participating atoms decreases, the focusing is expanded into a larger angular region, appearing less intense. The rise in I_{BS}(As) at $\alpha = 16°$ is strongly reduced upon hydrogenation. This effect comes from the decrease of the distance between first and second layer of As atoms from 0.223 nm for the clean surface to 0.18 nm for the hydrogenated surface [21].

Fig. 5 shows the intensity vs. α dependence for 4 keV Ar^+ backscattered from clean and hydrogenated W(211) surfaces [19]. The incidence scan was measured along $\delta = 24°$ (with respect to the $[01\bar{1}]$ azimuth, inset of Fig. 7).

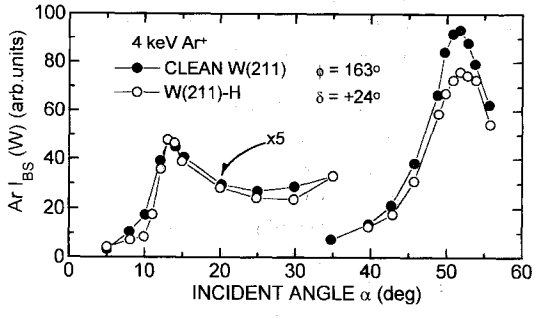

Fig. 5. Neutral plus ion intensity for 4 keV Ar backscattering from the clean and hydrogenated W(211) surfaces vs. the glancing angle [19].

Along this direction a change in the first-second layer spacing of 0.01 nm should result in a change of the position of the I_{BS}(W) steep rises of 2–3° [19]. We see in the figure that this difference is smaller than 1° (of the order of the experimental error). A similar behavior was found for other azimuthal directions, suggesting that contrary to the case of GaAs(110) the adsorbed H produces neither reconstruction of the surface nor changes of its relaxation.

There are several approaches to analyze the experimental data, these go from simple calculations of the shadow cones [6,7,30], to full calculations of the projectile and recoil trajectories using codes that allow the description of multiple collision events and delineate the contribution from several atomic layers [6,31,32]. For many applications it is sufficient to calculate only the shadowing and focusing regions and plot them in the incidence and azimuthal angles [10,21,33]. To exemplify this method, we show in Fig. 6(a) the shadowing regions corresponding to collisions of 6 keV Ne^+ with the As and Ga atoms of the relaxed GaAs(110) first layer, together with the experimental critical angles (full symbols) measured from incidence scans similar to that shown in Fig. 4(a). The critical angles are defined at 70% of the I_{BS} sharp rises [21]. The shadowing regions were calculated with shadow cones given by Oen's formula [30], a calibrated ($C = 0.63$) Thomas–Fermi–Molière potential and a Ga–As interlayer spacing adjusted to reproduce the experimental points [21]. Each circle represents the angular region shadowed by a particular surface atom. Out of the circles the projectiles can be backscattered towards the detector from the speci-

fied layer through a single collision. At the edges of the outer circles focusing effects are present and the backscattered intensity should present a sharp rise. The best agreement between the experimental points and the focusing angles [21] was obtained for a GaAs(110) interlayer spacing of (0.066 ± 0.008) nm, which is in excellent agreement with values measured by other techniques. Fig. 6(b) shows the experimental critical angles obtained for the hydrogenated surface together with the shadowing regions that fit best the experimental points. The best fit corresponds to both Ga and As atoms positioned at the same height (within an error of 0.01 nm) and at a distance to the second layer of 0.18 nm [21], i.e., corresponding to a bulk terminated top layer with a small contraction.

In general it is considerably more difficult to determine the adsorption position of H than the atomic structure of the substrate. This is mainly because it is not possible to have backscattering from the H atoms; in this case the information is obtained from the variation of the intensity of H recoiled into forward angles with the glancing and azimuthal direction of incidence [6,7,34]. In recent years, the use of DRS has allowed to determine the H adsorption sites in several systems [19,34–38]. Fig. 7(a) shows the intensity of H recoiling at forward angles ($\phi = 45°$) vs. the incident angle α induced by bombardment of the hydrogenated W(211) surface with Ar^+ ions [19]. Along the $[01\bar{1}]$ and $[11\bar{3}]$ directions (inset of Fig. 7) the H recoil intensity present a pronounced maximum at low α and then remains low and structureless up to $\alpha = 45°$ (the cutoff value). Because of the forward scattering geometry the maximum at low α is formed by both true direct recoils and surface recoils (i.e., coming from multiple collisions), while the large α contribution comes mainly from true DR processes [19]. The lack of other H DR peaks for intermediate α indicates that there is no H buried in subsurface layers [19].

As it can be seen in Fig. 7(b), the critical angle for recoiling H along the $[1\bar{1}\bar{1}]$ direction appears at larger angles. This critical angle is determined by focusing of the

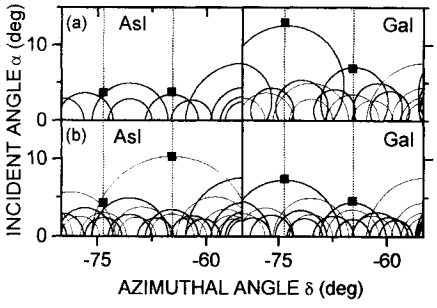

Fig. 6. Shadowing regions and experimental critical angles (■) for 6 keV Ne^+ backscattering from the clean (a) and hydrogenated (b) top GaAs(110) layer. The vertical lines indicate the span of the incidence scan.

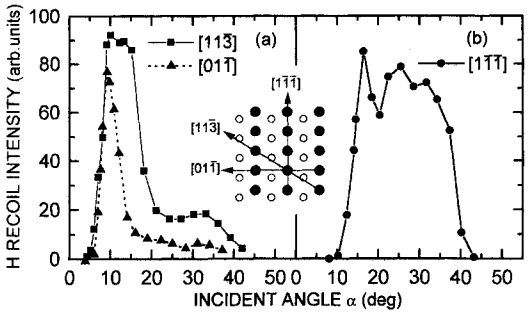

Fig. 7. H recoil intensity induced by 2 keV Ar^+ ions vs. the incident angle along the three azimuths indicated in the top view of the H:W(211) surface.

projectile trajectories by close packed H atoms. From an estimation of this focusing effect and the experimental critical angles measured for both Ar and Ne projectiles, a distance between two adjacent H atoms of ~ 0.27 nm was obtained [19]. This distance is similar to the interatomic distance for the W(211) surface along the $[1\bar{1}\bar{1}]$ direction, indicating a coverage of 1 ML. From the observed dependence of the H recoil energy and intensity with the incidence and azimuthal angles it was proposed [19] that the adsorbed H atoms reside in a band that is located along the $[1\bar{1}\bar{1}]$ troughs and at 0.057 nm above the first layer W atoms. No evidence was found for a preferential site within the band, which is in agreement with effective medium theory that predict H dispersion above the $[1\bar{1}\bar{1}]$ troughs due to thermally activated vibrational motion. A similar trend was found for H adsorption on Ru at 300 K [36], while for H adsorption on Ni [37], Si [38] and Pt stepped surfaces [34], localized sites were proposed.

5. Ion-surface electron exchange processes

The understanding of the mechanisms determining the ion fractions in the scattered and recoiled particles has progressed enormously during the last decade [3,4,6,7,39–41], leading to the proposal of promising applications [7,42]. TOF methods allow the measurement of both ion plus neutral and only neutral spectra, and from their difference the ion spectra can be obtained. Fig. 8 shows such TOF spectra for 6 keV Ne^+ backscattering from (a) clean and (b) hydrogenated GaAs(110) surfaces. A direction of measurement $(\alpha, \delta) = (8.5, 64.7)°$ was chosen which maximize the single backscattering from first Ga and As top layers. Deeper layers are within the shadow cone of the top layer atoms. The outgoing trajectory is 8.5° from the surface normal. We first note the sensitivity of the ion fractions with the colliding target element; the ion fractions coming from quasi-single Ne–Ga collisions are ~ 50% while those coming from Ne–As collisions are ~ 27% (obtained after a linear substraction of the multiple scatter-

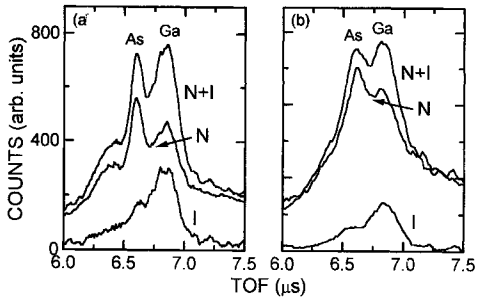

Fig. 8. Neutral plus ion (N+I), only neutral (N) and only ion (I) spectra for 6 keV Ne^+ backscattering from the clean (a) and hydrogenated (b) GaAs(110) surfaces.

ing contribution). This is the result of two combined effects, first, in the clean GaAs surface there are less electrons around the Ga atoms available for projectile neutralization, and second there is a quasi-resonant charge exchange process between the Ga 3d and Ne 2p levels that is not present in the Ne–As collision [39]. We can see in Fig. 8(b) that after hydrogen adsorption, the Ne ion fractions are reduced to 15 and 45% for Ne–As and Ne–Ga collisions, respectively. Since a similar behavior in the Ne ion fractions has been observed along other directions and the violent Ne–As and Ne–Ga collisions are the same for the clean and the hydrogenated surface, the observed change in the ion fraction should be related to the change induced by the adsorbed H on the chemical environment of the substrate atoms.

6. Summary

We have discussed the use of ion scattering and recoiling spectroscopy to obtain information about the adsorption of H on crystalline surfaces. In particular we have compared the H adsorption on W(211) and on GaAs(110). The measurement of H recoils allows monitoring of the H coverage and its dependence with the surface temperature. The time-of-flight distributions of the projectile backscattered intensities are very sensitive to the changes produced in the substrate atomic structure upon H adsorption. Their variation with the incidence direction indicates that H produces no major effect on the W(211) surface while it is efficient to remove the surface relaxation on GaAs(110). Finally, we have shown that the ion fractions obtained for Ne projectiles backscattered from the GaAs(110) surface are highly sensitive to the presence of adsorbed H.

Acknowledgements

O.G. gratefully acknowledges Professor Rabalais for many helpful discussions. This material is partially supported by CONICET (PID 3292/92), Fundación Antorchas (A13396/1) and Cooperativa de Electricidad Bariloche.

References

[1] D.P. Woodruff, T.A. Delchar, Modern Techniques of Surface Science, Solid State Science Series (Cambridge, 1994).
[2] L.C. Feldman, J.W. Mayer, Fundamentals of Surface and Thin Film Analysis (Elsevier, New York, 1986).
[3] J.W. Rabalais, CRC Crit. Rev. Solid State Mater. Sci. 14 (1988) 319.
[4] W. Eckstein, Nucl. Instrum. Methods B27 (1987) 78.
[5] T.M. Buck, G.H. Wheatly, D. Jackson, Nucl. Instrum. Methods 218 (1983) 257.
[6] H. Niehus, W. Heiland, E. Taglauer, Surf. Sci. Rep. 17 (1993) 213.
[7] J.W. Rabalais, Surf. Sci. 299&300 (1994) 219.
[8] M. Aono, C. Oshima, S. Zaima, S. Otani, Y. Ishizawa, Jpn. J. Appl. Phys. 20 (1981) L829.
[9] Th. Fauster, Vacuum 38 (2) (1988) 129.
[10] S.H. Overbury, Nucl. Instrum. Methods B27 (1987) 65.
[11] M.H. Mintz, I. Jacob, D. Shaltiel, in: Topics in Applied Physics, Vol. 67, ed. L. Schlapbach (Springer, Berlin, 1992).
[12] M.S. Hammond, J.A. Schultz, A.R. Krauss, J. Vac. Sci. Technol. 13 (3) (1995) 1136.
[13] H. Niehus, E. Bauer, Rev. Sci. Instrum. 46 (9) (1975) 1275.
[14] S.B. Luitjens, A.J. Algra, E.P.Th.M. Suurmeijer, A.L. Boers, Appl. Phys. 21 (1980) 205.
[15] K. Sumitomo, K. Oura, I. Katayama, F. Shoji, T. Hanawa, Nucl. Instrum. Methods B33 (1988) 871.
[16] M. Katayama, E. Nomura, N. Kanakama, H. Soejima, M. Aono, Nucl. Instrum. Methods B33 (1988) 857.
[17] Y. Wang, M. Shi, J.W. Rabalais, Nucl. Instrum. Methods B90 (1994) 237.
[18] O. Grizzi, M. Shi, H. Bu, J.W. Rabalais, Rev. Sci. Instrum. 61 (1990) 740.
[19] M. Shi, O. Grizzi, H. Bu, J.W. Rabalais, Phys. Rev. B40 (1989) 10163.
[20] L.F. De Ferrariis, F. Tutzauer, E.A. Sánchez, R.A. Baragiola, Nucl. Instrum. Methods A281 (1989) 43.
[21] J.E. Gayone, R.G. Pregliasco, E.A. Sánchez, G.R. Gómez, O. Grizzi, Phys. Rev. B, in press.
[22] O. M'Hamedi, F. Proix, C. Sebenne, Semicond. Sci. Technol. 2 (1987) 418.
[23] F. Masson, C. Sass, O. Grizzi, J.W. Rabalais, Surf. Sci. 221 (1989) 299.
[24] R. Rye, B.D. Barford, P.G. Cartier, J. Chem. Phys. 59 (1973) 1693.
[25] H. Niehus, Ch. Hiller, G. Comsa, Surf. Sci. 173 (1986) L599.
[26] R. Spitzl, H. Niehus, B. Poelsema, G. Comsa, Surf. Sci. 239 (1990) 243.
[27] C. Roux, H. Bu, J.W. Rabalais, Surf. Sci. 259 (1991) 253.
[28] Y. Wang, M. Shi, J.W. Rabalais, Phys. Rev. B48 (3) (1993) 1678.
[29] J. Murakami, T. Hashimoto, I. Kusunoki, Vacuum 41 (1–3) (1990) 369.
[30] O.S. Oen, Surf. Sci. 131 (1983) L470.
[31] C.A. Severjns, G. Verbist, H.H. Bronsgerma, Surf. Sci. 279 (1992) 297.

[32] Y. Wang, S.V. Teplov, J.W. Rabalais, Nucl. Instrum. Methods B90 (1994) 237.
[33] L. Marchut, T.M. Buck, G.H. Wheatley, C.J. McMahon Jr., Surf. Sci. 141 (1984) 549.
[34] B.J. Koeleman, S.T. de Zwart, A.L. Boers, B. Poelsema, L.K. Verheij, Phys. Rev. Lett. 56 (1986) 1152.
[35] F. Shoji, K. Kashihara, K. Sumitomo, K. Oura, Surf. Sci. 242 (1991) 422.
[36] J. Schulz, E. Taglauer, P. Feulner, D. Menzel, Nucl. Instrum. Methods B64 (1992) 588.
[37] H. Bu, C. Roux, J.W. Rabalais, Surf. Sci. 271 (1992) 68.
[38] M. Shi, Y. Wang, J.W. Rabalais, Phys. Rev. B48 (3) (1993) 1689.
[39] W. Heiland, in: Interactions of Charged Particles with Solid and Surfaces, eds. A. Gras Martí et al. (Plenum, New York, 1991) p. 253.
[40] D.J.O. Connor, Y.G. Shen, J.M. Wilson, R.J. Mac Donald, Surf. Sci. 197 (1988) 277.
[41] R. Souda, K. Yamamoto, W. Hayami, T. Aizawa, Y. Ishizawa, Phys. Rev. B51 (1995) 4463.
[42] C.C. Hsu, H. Bu, A. Bousetta, J.W. Rabalais, Phys. Rev. Lett. 69 (1) (1992) 188.